Synthesis and Proton-Coupled Electron-Transfer Reaction of Self-Assembled Monolayers of a Ruthenium(II) Complex Containing Tridentate 2,6-Bis(benzimidazol-2-yl)pyridine on a Gold Surface: Comparison of Acid/Base Chemistry with Bulk Solution Chemistry

Masa-aki Haga,*,† Hun-Gi Hong,‡ Yoichi Shiozawa,† Yasushi Kawata,† Hideaki Monjushiro,§ Tsuyoshi Fukuo,‖ and Ryuichi Arakawa‖

Integrated Inorganic Material Chemistry Laboratory, Department of Applied Chemistry, Faculty of Science and Engineering, Chuo University, 1-13-27 Kasuga, Bunkyo-ku, Tokyo 112-8551, Japan, Graduate School of Science, Osaka University, Machikaneyama-cho, Toyonaka, Osaka 560, Japan, Department of Chemistry, Sejong University, Seoul 143-747, Korea, and Department of Applied Chemistry, Kansai University, 3-3-35, Yamate, Suita, Osaka 564-8680, Japan

The self-assembly and electrochemical properties of a novel Ru(bimpyH$_2$) complex functionalized by disulfide on a polycrystalline gold electrode (bimpyH$_2$ = bis(benzimidazol-2-yl)pyridine) were characterized by means of MALDI-TOF mass spectrometry, XPS, and cyclic voltammetry. The Ru complex monolayers exhibit a quasi-reversible Ru(III/II) oxidation at +0.66 V vs SCE in 0.1 M HClO$_4$ aqueous solution. The shape of the cyclic voltammograms for Ru(III/II) couple is strongly dependent on the surface coverage, and is close to the ideal voltammogram when the Ru neat monolayers are diluted by octanethiol. The oxidation potential of the Ru complex mixed monolayers with octanethiol shows a linear dependence on solution pH, indicating that the proton-coupled oxidative reactions occurred on the gold surface. The pK_a values for the Ru mixed monolayers on the gold surface were obtained as pK_{a1} = 6.0 and pK_{a2} = 7.8 for the Ru(II) state and ∼1.5 and 3.4 for the Ru(III) state from the $E_{1/2}$−pH plots. The pK_a values of the Ru(bimpyH$_2$) group on the gold surface are a little smaller than those of [Ru(dmbimpy)(bimpyH$_2$)]$^{2+}$ (dmbimpy = bis(1-methylbenzimidazol-2-yl)pyridine) in the bulk solution. These disulfide-functionalized Ru(bimpyH$_2$) complex monolayers on the gold surface can act as an electrochemical pH probe on the surface.

Introduction

Protons play an important role in bioenergetic systems such as proton-coupled electron-transfer reactions and proton pumps through biomembranes.[1] Proton transfer and proton gradients are of fundamental importance in bioenegetics. In a photosynthetic membrane, the electron flow can be coupled directly to the electrolytic flow of protons across the membrane to maintain the proton gradients. Thus, the combination of proton transfer and electron transfer is attractive not only in developing the biomimic catalysts[2] but also in designing biomimic molecular electronics based on the proton movements.[3,4] Many examples of proton-coupled electron-transfer reactions have been reported in the field of inorganic chemistry.[5,6] As part of our study of proton-induced tuning or switching of chemical properties in Ru complexes, we earlier reported a proton-coupled electron-transfer reaction in the mononuclear Ru(bimpyH$_2$)$_2$ complex[7] and dinuclear and tetranuclear Ru complexes bridged by 2,2′-bis(2-pyridyl)bibenzimidazole.[8,9] A proton-coupled electron-transfer reaction can be expressed by a square scheme involving electron-transfer and proton-transfer equilibria. Such a system can be graphically described by a Pourbaix diagram, which gives us the acid dissociation constant, pK_a, for different oxidation states. Once Ru complexes exhibiting proton-coupled redox reactions are immobilized on a surface, direct information for surface acidity can be obtained from the analysis of their Pourbaix diagrams.

The self-assembly of organic thiols or disulfides on a gold surface is a well-established method to fabricate highly organized stable monolayers.[10,11] The exceptionally high affinity of gold for thiolates allows incorporation of virtually any functional group in such monolayers.[12] These well-defined and ordered

* To whom correspondence should be addressed. E-mail: mhaga@chem.chuo-u.ac.jp.
† Chuo University.
‡ Sejong University.
§ Osaka University.
‖ Kansai University.

(1) Link, T. A. In *Electron and Proton Transfer through the Mitochondrial Respiratory Chain*; Muller, A., Ratajczak, H., Junge, W., Diemann, E., Eds.; Elsevier Science Publishers: Amsterdam, 1992; Vol. 78, p 197.
(2) Nakamoto, M.; Tanaka, K.; Tanaka, T. *Bull. Chem. Soc. Jpn.* **1988**, *61*, 4099.
(3) Niemz, A.; Rotello, V. M. *Acc. Chem. Res.* **1999**, *32*, 44.
(4) Tam-Chang, S.-W.; Mason, J.; Iverson, I.; Hwang, K.-O.; Leonard, C. *Chem. Commun.* **1999**, 65.
(5) Thorp, H. H. *Chemtracts: Inorg. Chem.* **1991**, *3*, 171.
(6) Trammell, S. A.; Wimbish, J. C.; Odobel, F.; Gallagher, L. A.; Narula, P. M.; Meyer, T. J. *J. Am. Chem. Soc.* **1998**, *120*, 13248.

(7) Xiaoming, X.; Haga, M.; Matsumura-Inoue, T.; Ru, Y.; Addison, A. W.; Kano, K. *J. Chem. Soc., Dalton Trans.* **1993**, 1993.
(8) (a) Bond, A. M.; Haga, M. *Inorg. Chem.* **1986**, *25*, 4507. (b) Haga, M.; Ano, T.; Kano, K.; Yamabe, S. *Inorg. Chem.* **1991**, *1991*, 3843.
(9) Haga, M.; Ali, M. M.; Koseki, S.; Fujimoto, K.; Yoshimura, A.; Nozaki, K.; Ohno, T.; Nakajima, K.; Stufkens, D. J. *Inorg. Chem.* **1996**, *35*, 3335.
(10) Ulman, A. *Chem. Rev.* **1996**, *96*, 1533.
(11) Finklea, H. O. In *Electroanalytical Chemistry*; Bard, A. J., Rubinstein, I., Eds.; Dekker: New York, 1996; Vol. 19, p 109.
(12) Porter, M. D.; Bright, T. B.; Allara, D. L.; Chidsey, C. E. D. *J. Am. Chem. Soc.* **1987**, *109*, 3559−3568.

surfaces have been used to study electron-transfer kinetics and interfacial phenomena. A variety of electroactive functional groups in the attached molecule have been explored in an effort to understand and control the properties of solid interfaces such as wetting, corrosion, and adhesion.[13−15] The types of electroactive headgroups with transition-metal complexes attached through thiol tethers to gold have been limited, and the majority of studies used the ferrocenium/ferrocene couple or $[Ru(NH_3)_5L]^{3+/2+}$.[16−22] Recently, a molecular-sized pH probe comprised mixed self-assembled monolayers (SAMs) of *p*-hydroquinone and ferrocenethiol, in which a proton-coupled electron-transfer reaction on the *p*-hydroquinone moiety created a pH-sensng moiety.[23] Furthermore, galvinol-substituted alkanethiols were reported to exhibit proton-coupled redox reactions and were applied for the pH-gated single-electron tunneling devices.[24] Detailed studies on the ionization of acidic groups in organic compound SAMs indicated that the formation of a charged group from a neutral one is more difficult by at least 2 pH units than the corresponding reaction in solution.[17,18,25,26] However, studies of the surface chemistry from the viewpoint of proton-coupled electron-transfer system are relatively sparse.[6,14,27] In this paper, we examined the proton-coupled electron-transfer reactions of Ru−bimpyH₂ on a gold surface by introducing a new anchoring disulfide ligand, 2,6-bis(1-thioalkylbenzimidazol-2-yl)pyridine (Scheme 1), to obtain pK_a values for Ru SAM complexes or monitor the local pH in the SAM systems, compared with those in bulk solution.

Experimental Section

Materials. 2,6-Pyridinedicarboxylic acid (Nacalai) and ruthenium trichloride trihydrate (N.E. Chemcat) were used without further purification. Dimethylformamide (DMF) was HPLC grade. All other supplied chemicals were of standard reagent grade quality.

Synthesis. The compounds bis(benzimidazol-2-yl)-pyridine (bimpyH₂),[28] bis(1-methylbenzimidazol-2-yl)pyridine (dmbimpy),[28] Ru-(bimpyH₂)Cl₃,[29] and [Ru(dmbimpy)(bimpyH₂)](PF₆)₂[7] were prepared as reported previously.

Synthesis of the Anchoring Ligand: 2,6-Bis(1-(8-bromooctyl)-benzimidazol-2-yl)pyridine. NaH (oil dispersion, 58%; 0.26 g, 7.0

Scheme 1. Structures of the Ru Complexes

[Ru(dmbimpy)(bimpyH₂)]²⁺

[Ru(L18)(bimpyH₂)]²⁺

[Ru(dtbimpy)(bimpyH₂)]²⁺

Ru(bimpyH₂) SAM
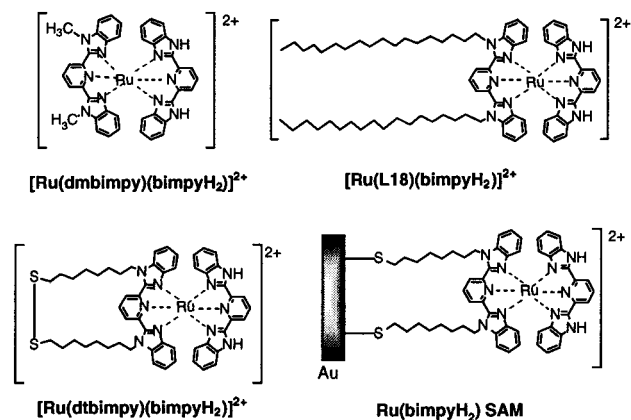
mmol) was washed with dry *n*-pentane and then suspended in dried DMF (14 mL). To this suspension was added 2,6-bis(benzimidazol-2-yl)pyridine (1.0 g, 3.2 mmol) under nitrogen atmosphere, and the mixture was heated to 80 °C for 2 h, during which time the suspension slowly dissolved and became a yellow homogeneous solution. The resulting solution, transferred to the dropping funnel by using a cannula techniques, was added to 1,8-dibromooctane (3.5 mL, 19.2 mmol) in DMF (15 mL) dropwise at room temperature and then heated to 100 °C for 2 h. After being cooled to room temperature, the solution was hydrolyzed with aqueous NH₄Cl (1 mol, 100 mL), and then extracted by CH₂Cl₂. The extract was washed with water, and then brine, dried on magnesium sulfate, and concentrated to half of its volume. The product was purified by column chromatography on a silica gel with ether/ethyl acetate. The desired compound, eluted as a third band, was obtained as an oil. Yield: 1.03 g (46%). Mass spectrum: $m/z = 613$ (M − Br + H)⁺); M = C₃₅H₄₄N₅Br₂. ¹H NMR (in CDCl₃): δ 1.05 (m), 1.63 (m), 1.71 (m), 3.25 (t), 4.70 (t), 7.37 (m), 7.46 (dd), 7.87 (dd), 8.06 (t), 8.32 (d).

2,6-Bis(1-(8-thioacetyloctylbenzimidazol-2-yl)pyridine. 2,6-Bis-(1-(8-bromooctylbenzimidazol-2-yl)pyridine (1.03 g, 1.5 mmol) was dissolved in dried THF (10 mL), and solid potassium thioacetate (1.5 g, 13 mmol) was added to the solution at room temperature. The solution was heated for 14 h at 50 °C. After being cooled to room temperature, the solution was hydrolyzed with aqueous NH₄Cl (1 mol, 100 mL), and then extracted by CH₂Cl₂. The extract was washed with water, and then brine, dried on magnesium sulfate, and concentrated to half of its volume. The product was purified by column chromatography on silica gel with ether/ethyl acetate, obtained as a pale yellow oil. Yield: 0.37 g (36%). Mass spectrum: $m/z = 683$ (M⁺), 640 ((M − Ac)⁺), 609 ((M − 2Ac)⁺); M = C₃₉H₄₉N₅O₂S₂. ¹H NMR (in CDCl₃): δ 1.03 (m), 1.53 (m), 1.71 (m), 2.72 (s), 4.69 (t), 7.37 (m), 7.46 (dd), 7.87 (dd), 8.06 (t), 8.32 (d).

Synthesis of Ru Complex [Ru(dtbimpy)(bimpyH₂)](PF₆)₂. A suspension of [Ru(bimpyH₂)Cl₃] (0.28 g, 0.54 mmol) was refluxed in ethylene glycol (40 mL) until complete dissolution. 2,6-Bis(1-(8-thioacetyloctyl)benzimidazol-2-yl)pyridine (0.37 g, 0.54 mmol) in toluene (6 mL) was then added to the solution, and heating was continued for a further 10 h, during which time the color of the solution changed from red-brown to dark brown. After being cooled to room temperature, a saturated aqueous solution of NH₄PF₆ was added dropwise to the concentrated solution, leading to the formation of a black precipitate. To keep the solution acidic, HCl (6 M) was added to the solution, and then the resulting precipitate was collected. Purification was affected by column chromatography on aluminum oxide with CH₃-CN. The desired mononuclear complex was eluted as a second blue-violet band. After addition of a drop of HCl, the eluate was evaporated to dryness. The crude product was recrystallized from CH₃CN/ether. Yield: 0.29 g (37%). During the synthetic manipulation of the complex, the formation of an S−S bond occurred as a result of the deacylation from the 2,6-bis(1-(8-thioacetyloctyl)benzimidazol-2-yl)pyridine moiety. Anal. Calcd for C₅₄H₅₆N₁₀RuS₂P₂F₁₂: C, 49.88; H, 4.34; N, 10.77. Found: C, 50.23; H, 4.68; N, 10.46. ESI mass spectrum: $m/z = 1009$ (M − 2PF₆ − H)⁺. M = C₅₄H₅₆N₁₀RuS₂P₂F₁₂. ¹H NMR (in CDCl₃):

(13) Ferrence, G. M.; Henderson, J. I.; Kurth, D. G.; Morgenstern, D. A.; Bein, T.; Kubiak, C. P. *Langmuir* **1996**, *12*, 3075.
(14) Beulen, M. W. J.; Huisman, B.-H.; van der Heijden, P. A.; van Veggel, F. C. J. M.; Simons, M. G.; Biemond, E. M. E. F.; de Lange, P. J.; Reinhoudt, D. N. *Langmuir* **1996**, *12*, 6170.
(15) Chechik, V.; Stirling, C. J. *Langmuir* **1998**, *14*, 99.
(16) Uosaki, K.; Sato, Y.; Kita, H. *Langmuir* **1991**, *7*, 1510.
(17) Ryswyk, H. V.; Turtle, E. D.; Watson-Clark, R.; Tanzer, T. A.; Herman, T. K.; Chong, P. Y.; Waller, P. J.; Taurug, A. L.; Wagner, C. E. *Langmuir* **1996**, *12*, 6143.
(18) Lee, T. R.; Carey, R. I.; Biebuyck, H. A.; Whitesides, G. M. *Langmuir* **1994**, *10*, 741.
(19) Offord, D. A.; Sachs, S. B.; Ennis, M. S.; Eberspacher, T. A.; Griffin, J. H.; Chidsey, E. D.; Collman, J. P. *J. Am. Chem. Soc.* **1998**, *120*, 4478.
(20) Campbell, D. J.; Herr, B. R.; Hulteen, J. C.; Van Duyne, R. P.; Mirkin, C. A. *J. Am. Chem. Soc.* **1996**, *118*, 10211.
(21) Uosaki, K.; Kondo, T.; Zhang, X.-Q.; Yanagida, M. *J. Am. Chem. Soc.* **1997**, *119*, 8367.
(22) Imahori, H.; Yamada, K.; Hasegawa, M.; Taniguchi, S.; Okada, T.; Sakata, Y. *Angew. Chem.* **1997**, *36*, 2626.
(23) Hickman, J. J.; Ofer, D.; Laibinis, P. E.; Whitesides, G. M.; Wrighton, M. S. *Science* **1991**, *252*, 688.
(24) Brousseau, L. C.; Zhao, Q.; Shulz, D. A.; Feldheim, D. L. *J. Am. Chem. Soc.* **1998**, *1998*, 7645.
(25) Rowe, G. E.; Creager, S. E. *Langmuir* **1991**, *7*, 2307.
(26) Shimazu, K.; Teranishi, T.; Sugihara, K.; Uosaki, K. *Chem. Lett.* **1998**, 669.
(27) Maskus, M.; Abruna, H. D. *Langmuir* **1996**, *12*, 4455.
(28) Addison, A. W.; Burke, P. J. *J. Heterocycl. Chem.* **1981**, *18*, 803.
(29) Haga, M.; Kato, N.; Monjushiro, H.; Wang, K.; Hossain, M. D. *Supramol. Sci.* **1998**, *5*, 337.

δ 1.05 (m), 1.63 (m), 1.71 (m), 3.25 (t), 4.70 (t), 7.37 (m), 7.46 (dd), 7.87 (dd), 8.06 (t), 8.32 (d).

Preparation of the Gold Electrode and Monolayers of the Ruthenium(II) Complex on the Gold Surface. Gold electrodes were prepared by vacuum deposition onto a borosilicate glass slide (1 in. × 3 in.). The glass slides were precleaned by being immersed in a hot "piranha" solution (30% H_2O_2:98% H_2SO_4 = 1:3 v/v) for 2 h, rinsed with ultrapure water, and dried with a nitrogen stream. **Caution:** *Piranha solution reacts violently, even explosively, with organic materials, and it should not be stored in sealed containers or combined with significant quantities of organic material.* Then the glass slides were immersed into a silanization solution (3-mercaptopropyltrimethoxysilane:anhydrous toluene = 1:99 v/v) for 24 h to form an adhesion layer for the gold film. After being washed with fresh toluene and dried with a nitrogen stream, the substrate was transferred to a vacuum chamber. The deposition was carried out in a vacuum of ca. 10^{-6} Torr with high-purity gold (99.99%). The film thickness was ca. 200 nm, and the deposition rate was ca. 0.1 nm/s. The temperature of the substrate was kept at 300 °C during the deposition. The gold electrodes were deposited onto the silanized glass slide through an aluminum mask with six uniformly spaced circular holes (0.250 cm in radius) and narrow slits for electrical contact. The geometrical area of the individual gold disk electrode was typically 0.196 cm^2. The roughness factors for these electrodes were measured in the 1.1–1.2 range, and the actual surface areas were obtained from the slope of the linear plot of cathodic peak current vs (scan rate)$^{1/2}$ for the reversible reduction of $[Ru(NH_3)_6]^{3+}$. As previously reported, we have used for this purpose a diffusion coefficient of 7.5×10^{-6} cm^2 s^{-1} (at 25 °C in 0.1 M NaCl).[30] To make the electrical contact, the end of the gold slit was clamped with an alligator clip. The electrode was cleaned by being immersed into a warm piranha solution for 10 s and was cycled electrochemically between −0.20 and +1.20 V vs SCE in 0.5 M H_2SO_4 until the typical cyclic voltammogram of gold was obtained. The dried and precleaned gold electrode was soaked for 48 h in a 350 μM acetonitrile/ethanol solution of the Ru(II) complex and obtained the saturated surface coverage. Afterward, the electrode was thoroughly rinsed with fresh acetonitrile, ethanol, and water.

Physical Measurements. Electrochemical experiments were performed in a conventional three-electrode cell. The electrolyte solutions were prepared with deionized water purified to a resistivity of 18.2 $M\Omega$ cm^{-1} with a UHQ-III system (Elga Co.) and purged with argon before use. The Ru(II) complex-modified gold electrode, saturated calomel electrode (SCE), and Pt wire were used as working electrode, reference electrode, and counter electrode, respectively. The cyclic voltammetric measurements were conducted with a BAS 100/B electrochemical analyzer. $HClO_4$ (0.1 M) was typically used as electrolyte solution, the pH of the solution was adjusted with 1.0 M NaOH, and the ionic strength was maintained at 0.5 M by the addition of $NaClO_4$. The pH measurements were made with a TOA model HM-20E pH meter standardized with buffers of pH 4.01 and 6.89. A 50% acetonitrile–buffer mixture was also employed for the comparison of previous data for the relevant Ru–bimpyH$_2$ complexes.[7,8] Buffer systems and the pH ranges employed were as follows: $HClO_4$–$NaClO_4$, pH 0–2; Robinson–Britton buffer, pH 2–11. All cyclic voltammograms for the reductive desorption were measured at a scan rate of 100 mVs^{-1} in a deaerated 0.1 M KOH aqueous solution.

UV spectra were obtained on a Hitachi U-4000 or a U3210 spectrophotometer. Spectrophotometric titrations were performed in acetonitrile–water (1:1 v/v) solution, as described previously.[7,8] XPS spectra were measured on a VG Scientific ESCA Mark II photoelectron spectrometer with Mg Kα radiation as an excitation source. The binding energies of the peaks were referenced to the C 1s peak at 285.0 eV. Two different angles for the sample, 15° and 60° against the surface normal, were used for the angle-dependent XPS measurement. Mass spectrometric experiments were carried out with matrix-assisted laser desorption/ionization time-of-flight mass spectrometry (MALDI-TOF-MS), VISION 2000 (Finnigan MAT). A nitrogen pulse gas laser was used with a wavelength of 337 nm, a pulse duration of approximately 3 ns, a maximum pulse energy of 250 mJ, and a maximum repetition

Scheme 2. Synthetic Route of the Ruthenium Disulfide Complex
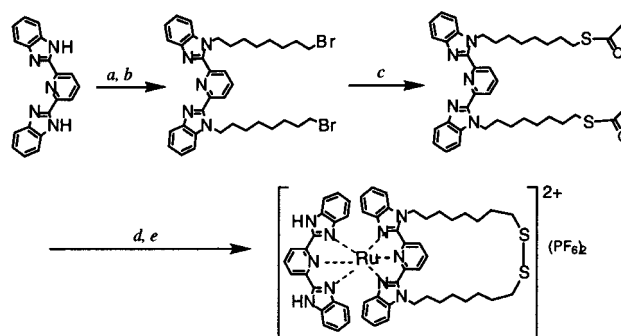
^{a} NaH in DMF, ∼100 °C, 5 h. ^{b}1,8-Dibromooctane, ∼100 °C, 3 h. ^{c}KSAc in THF, reflux, overnight. ^{d}Ru(bbimpyH$_2$)Cl$_3$ in ethylene glycol. ^{e}Saturated NH$_4$PF$_6$ aqueous solution.

rate of 10 Hz. The matrix used for the MALDI measurements was 10 mg/mL 2,5-dihydroxybenzoic acid (DHB) dissolved in an aqueous solution of 10% CH_3CN + 0.1% trifluoroacetic acid. A 0.3 mL sample of the matrix was placed on the SAM samples, and was dried in air. Two kinds of SAM samples were prepared for the MALDI measurement; one was Ru complex immobilized onto a Au layer (1000 Å) based on a stainless steel plate, the other on a glass plate. The MALDI spectra were obtained in the positive ion mode. The mass calibration was carried out with an oligopeptide (1251.7 Da).

Results and Discussion

Synthesis. The synthetic route to the anchoring ligand and its Ru complex is summarized in Scheme 2. The anchoring ligand, 2,6-bis(1-(8-thioacetyloctylbenzimidazol-2-yl)pyridine, was prepared in two steps, starting from 2,6-bis(benzimidazol-2-yl)pyridine. We had tried to prepare the Ru complex containing 2,6-bis(1-(8-thioacetyloctylbenzimidazol-2-yl)pyridine from the reaction of 2,6-bis(1-(8-thioacetyloctylbenzimidazol-2-yl)-pyridine with [Ru(bimpyH$_2$)Cl$_3$] in ethylene glycol/toluene. During the manipulation of the solution for this reaction under air, we observed S−S bond formation occurred as a result of deacylation, followed by air oxidation of the thiol groups. This was an unexpected reaction, but the resulting Ru complex was well characterized by the ^{1}H NMR, ESI-MS, and elemental analysis. This novel ruthenium disulfide complex was used as a surface-immobilized reagent.

Characterization of the Ru Complex-Modified Gold Electrode. The Ru complex was directly attached to the surfaces of gold substrates from acetonitrile/ethanol (1:1 v/v) mixed solution to form a SAM film. The XPS core level spectra for the Ru complex and the SAM of the Ru complex on the gold electrode were measured and are available as Supporting Information (Figure S1). The XPS spectrum for the powder of the Ru complex gave characteristic elemental signatures: S 2p, C 1s, Ru 3d, N 1s, F 1s, and P 2p lines. The Ru 3d$_{5/2}$ signal was observed at 281.3 eV, which is a typical value for Ru(II) complexes.[31,32] The S 2p peak was observed at ca. 163.5 eV, which coincides with that observed for S dimers in 4,4′-diaminodiphenyl disulfide.[33] Although the powder sample of the Ru complex clearly shows an F 1s peak at 686.3 eV and a P 2p peak at 163.7 eV, respectively, neither F 1s nor P 2p signals were observed for the SAM of the Ru complex on gold. This result implies that the PF$_6$ anion is not transferred on the gold

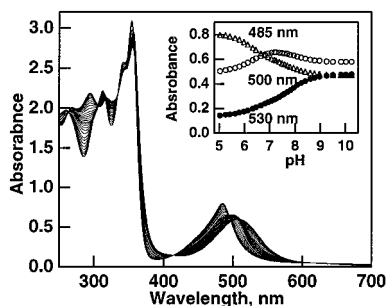(30) Gomez, M. E.; Li, J.; Kaifer, A. E. *Langmuir* **1991**, *7*, 1797.

(31) Brant, P.; Stephenson, T. A. *Inorg. Chem.* **1987**, *26*, 22.
(32) Shepherd, R. E.; Proctor, A.; Henderson, W. W.; Myser, T. K. *Inorg. Chem.* **1987**, *26*, 2440.
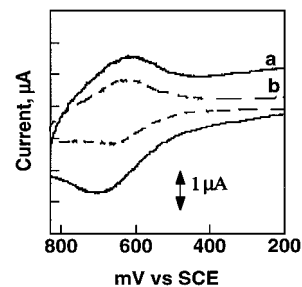(33) Golzhauser, A.; Panov, S.; Woll, C. *Surf. Sci.* **1994**, *314*, 849.

Figure 1. pH dependence of absorption spectra for [Ru(dmbimpy)-(bimpyH₂)](PF₆)₂ in CH₃CN/buffer (1:1 v/v) solution in the pH range from 5.03 to 9.82. The titration curves at different wavelengths are shown as an inset.

Figure 2. Cyclic voltammograms of [Ru(dtbimpy)(bimpyH₂)](PF₆) in aqueous 0.1 M HClO₄ solution at a sweep rate of 0.1 V/s at (a) a gold electrode coated with a monolayer of the Ru(II) complex only and (b) the same electrode of (a) after having been reimmersed for 2 days in a 0.5 mM ethanol solution of octanethiol.

substrate upon adsorption of the Ru complex. Therefore, it is suggested that deprotonation of the benzimidazolyl N−H group takes place to give the SAM of the neutral charged Ru complex. Deprotonation of the benzimidazolyl N−H groups is also supported by the fact that a shoulder appears on the low binding energy side of the N 1s peak in the spectrum of the SAM of the Ru complex which is assigned to the deprotonated benzimidazolyl N⁻ group. Except for the F 1s and P 2p peaks there is no significant difference in the peak intensity ratio of the component elements between the powder and the SAM film of the Ru complex. However, both F 1s and P 2p peaks were observed when small amounts of HPF₆ were added to the SAM solution. Therefore, the degree of protonation of the Ru−bimpyH₂ complex on the gold surface is drastically influenced by the SAM-depositing condition and solvents.

The angular dependence of the XPS spectra was measured at the collecting angles of 15° and 60° against the surface normal. The relative intensity ratio of both S 2p to N 1s and S 2p to Ru 3d$_{5/2}$ is smaller at lower angles (60°) against the surface normal, although the ratio of Ru 3d$_{5/2}$ to N 1s is almost constant. In general, the intensity of the XPS signal, I, depends on the collecting angle θ as $I \propto \exp(-d/L \cos \theta)$, where d is the depth from the sample surface where the element of interest is present and L is the attenuation length of the photoelectrons for the corresponding signal. Therefore, this angular dependence reveals that the S atom is located more deeply than that of the Ru ion: that is, the disulfide site is more closely located to the gold surface than the Ru site.

Characterization of the Ru SAM surface was carried out using MALDI-TOF-MS. The MALDI spectrum of the SAMs supported on the gold-deposited glass plate is given in the Supporting Information (Figure S2). The peak at m/z 1009 corresponds to the molecular ion $[M − 2X^- − H^+]^+$ (X = PF₆), which strongly indicates the presence of the Ru complex on the Au surface. It is noteworthy that no fragment ion with loss of the ligand was observed in the MALDI ionization process of this SAM sample. In addition, ion production was found to be due to the preferred bond dissociation between thiol and the Au surface. In the case of the SAM sample supported on the Au-deposited stainless steel plate, the dimer complex peak [2M − 4X⁻ − H⁺]⁺ was observed as well as the molecular ion peak.

Comparative Acid/Base Chemistry of Ru(bpimH₂) Complexes in Different Microenvironments. UV Spectra. The UV absorption spectrum of the Ru complex [Ru(dmbimpy)-(bimpyH₂)]²⁺ in CH₃CN/buffer (1:1 v/v) at pH 5 shows an MLCT band at 485 nm and $\pi\pi^*$ bands at 354, 341, and 312 nm. The MLCT band is sensitive to the solution pH; the MLCT band appeared at 485 nm below pH < 5, 500 nm in the pH range of 5 < pH < 7.5, and 508 nm above pH 7.5 (Figure 1).

From this spectral change on pH, the values of the acid dissociation constant, pK_a, were determined as pK_{a1} = 6.35 and pK_{a2} = 7.87. A similar spectral change was observed for [Ru-(dtbimpy)(bimpyH₂)]²⁺ in CH₃CN/buffer (1:1 v/v), which leads to the evaluation of the pK_a values as pK_{a1} = 5.70 and pK_{a2} = 7.33, which are comparable to the acid dissociation constants of analogous [Ru(L18)(bimpyH₂)]²⁺ (L18 = 2,6-bis(1-octadecylbenzimidazol-2-yl)pyridine) in a micelle solution (10 mM Triton/0.1 M Na₂SO₄) (pK_{a1} = 5.35 and pK_{a2} = 6.94).[33] It is well-known that the pK_a values are sensitive for the microenvironment. Therefore, the similarity of the pK_a value of [Ru-(dtbimpy)(bimpyH₂)]²⁺ to that of [Ru(L18)(bimpyH₂)]²⁺ in the micelle solution suggests the complex [Ru(dtbimpy)(bimpyH₂)]²⁺ may form the micelle-like mesostructure in CH₃CN/buffer solution.

Cyclic Voltammetry. In CH₃CN/Buffer Solution. The cyclic voltammogram of [Ru(dmbimpy)(bimpyH₂)]²⁺ in CH₃-CN/buffer (1:1 v/v) solution at pH 2.0 shows one reversible oxidation process at +0.69 V vs SCE. The cyclic voltammogram of [Ru(dmbimpy)(bimpyH₂)]²⁺ reveals a strong pH dependence as shown in the Supporting Information (Figure S3), indicating that proton-coupled electron-transfer reaction also occurs in this complex. As the solution pH increases, the formal Ru(III/II) potential gradually shifts in the negative direction, which is exactly due to the deprotonation of the NH imino proton of the tridentate bimpyH₂ ligand of the Ru(II) complex.

For the general reversible electrode reaction

$$Ox + ne^- + mH^+ = Red$$
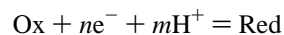
where Ox = oxidized species and Red = reduced species, the Nernst equation can readily be expressed as

$$E_{1/2} = E^{\circ\prime} - 0.059 \frac{m}{n}(\text{pH})$$

where $E_{1/2}$ is the half-wave potential and $E^{\circ\prime}$ is the formal electrode potential. From a plot of oxidation potential vs pH (Pourbaix diagram) for this complex, we can obtain the pK_a values as pK_{a1} = 6.35 and pK_{a2} = 8.10, which are consistent with those from spectrophotometric titration described in the previous section.

The SAM on a Gold Surface. Figure 2a shows a typical cyclic voltammogram of the Ru(II) complex SAM on a gold electrode in 0.1 M HClO₄. This voltammetric wave is assigned to the redox reaction of the immobilized Ru(III/II) couple, compared to the oxidation potential of analogous Ru complexes such as [Ru(dmbimpy)(bimpyH₂)]²⁺ and [Ru(bimpyH₂)₂]²⁺ in CH₃CN/buffer (1:1 v/v) solution.[7] The neat monolayer film was prepared from a CH₃CN/ethanol solution containing only the

Ru(II) complex. For this film, the characteristic surface formal Ru(III/II) potential appeared at +0.66 V vs SCE in aqueous 0.1 M HClO$_4$ solution, and its redox peak width at half-maximum is ca. 150 mV, significantly larger than the Nernstian width of 90 mV. The peak current of the cyclic voltammogram is proportional to the scan rate in the range from 10 to 200 mV s^{-1}, indicative of the redox reaction of the surface-immobilized species. In this voltammogram, a relatively large charging current was observed. The surface coverage of the immobilized Ru(II) complex molecules was determined by integrating the oxidation current peak assuming a one-electron redox mechanism. The value of surface coverage obtained from the voltammogram in Figure 2a is 1.8×10^{-10} mol/cm^2, which corresponds to 1.1×10^{14} molecules/cm^2. From the CPK model, the diameter of [Ru(bimpyH$_2$)$_2$]$^{2+}$ is ca. 1.2 nm, and the surface density at maximum coverage should therefore be about 0.9×10^{14} molecules/cm^2 (or 1.5×10^{-10} mol/cm^2) on the basis of the projected area of 1.13 nm^2/molecule. The surface density obtained in Figure 2a is slightly larger than the theoretical value for a monolayer of the Ru(II) complex disulfide. This indicates that the electroactive film contains fairly dense monolayers of the Ru(II) complex. Treatment of this modified Au electrode with octanethiol by reimmersing it for 2 days in the ethanol solution changed the shape of the voltammogram with a smaller double-layer charging current (Figure 2b). Integration of the charge gives a coverage of 0.5×10^{-10} mol/cm^2, which is one-third of a monolayer coverage for the Ru(II) complex molecule. These facts demonstrate that the substitution of the Ru(II) complex molecules with octanethiol on the gold surface produces a well-mixed and -ordered structure of the Ru(II) complex monolayer. For the mixed Ru SAM film with coadsorption of the diluent octanethiol, the oxidation and reduction peaks are quite symmetric, and the peak width (100 mV) at half-maximum is quite close to that of the Nernstian value. The surface coverage of 0.8×10^{-10} mol/cm^2 is typically obtained when the mole fraction of the Ru(II) complex is 0.88 in the thiol deposition solution. We chose octanethiol as a diluent because its alkyl chain length is equivalent to that of the tethered Ru(II) complex disulfide. The coadsorption of the diluent molecule not only makes the metal redox center fully extended to the electrode surface but also improves structural ordering by increasing the packing density of the Ru complex monolayer.

Most of the cyclic voltammograms for the surface-confined Ru(II) complex in this study show that the double-layer capacitance is increased when the metal redox center is oxidized. This might be due to the influx of counter ion into the monolayer to maintain the electroneutrality at the film/solution interface.

To obtain further information about the microenvironment around the Ru SAM, cyclic voltammograms for the reductive desorption of both pure Ru SAM and the mixed SAM with octanethiol adsorbed on the Au substrate were measured in 0.1 M KOH aqueous solution. Figure 3 shows a comparison of the cyclic voltammograms for the reductive desorption of the pure Ru SAM, the mixed Ru SAM with octanethiol, and the pure octanethiol SAM. Two reductive desorption peaks, I and II, of the pure Ru SAM appeared at −0.72 and −1.14 V vs SCE, while only one desorption peak, II, of the pure octanethiol SAM appeared at −1.08 V. When the mixed Ru SAM was prepared from an acetonitrile/ethanol solution containing [Ru(dtbimpy)-(bimpyH$_2$)]$^{2+}$ and octanethiol with a 1:1 molar ratio, two desorption peaks, I and II, were observed at −0.89 and −1.11 V. Desorption peak I is shifted 170 mV to negative potential; however, peak II is slightly shifted 30 mV in the positive direction. Furthermore, the cyclic voltammogram of the de-
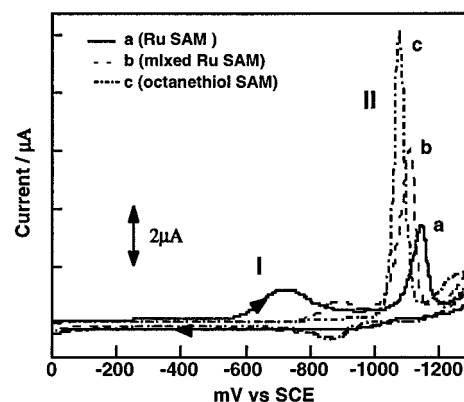

Figure 3. Cyclic voltammograms for the reductive desorption of (a) the pure Ru SAM, (b) the mixed Ru SAM with octanethiol, and (c) the pure octanethiol SAMs in 0.1 M KOH aqueous solution at a scan rate of 0.1 V/s.

Scheme 3. Proposed Adsorption and Desorption Processes of [Ru(dtbimpy)(bimpyH$_2$)]
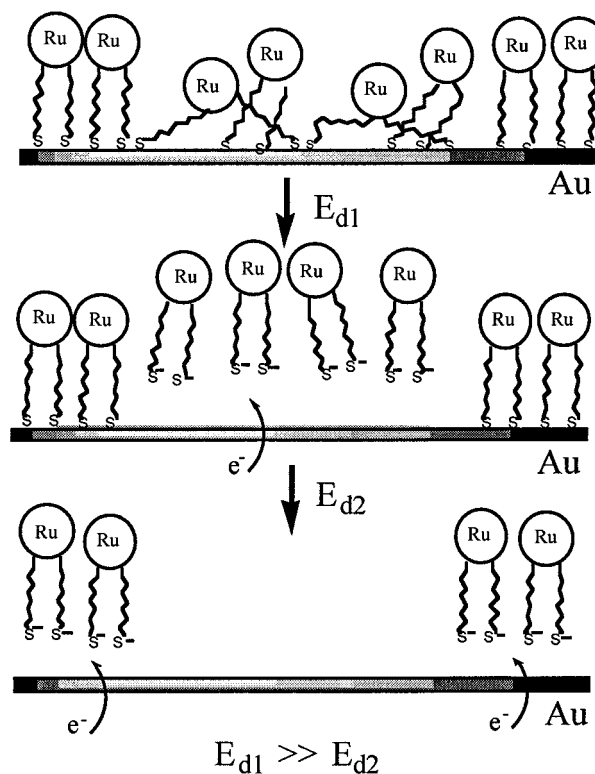
sorption process of the pure Ru SAM shows a strong dependence on the immersion time. In the early stage of the Ru SAM adsorption process, the peak II area at −1.08 V is ca. 5 times larger than that of peak I at −0.78 V. During the time course of the adsorption, peak I becomes larger compared to peak II, and moves in the positive direction, but the position of peak II is almost constant. The appearance of two peaks, I and II, indicates the existence of two different microenvironments with different stability in the desorption process; i.e., the second desorption process, II, possesses a more stabilizing environment than the first one, I. Two different molecular arrangements are considered for peaks I and II, i.e., a randomly oriented disordered structure and a well-ordered domain structure with a weak intermolecular interaction through the (benzimidazol-2-yl)pyridine moiety in [Ru(dtbimpy)(bimpyH$_2$)]$^{2+}$, respectively (Scheme 3). Recently, we have reported the domain formation of an analogous Ru complex with a long alkyl chain, [Ru(L18)-
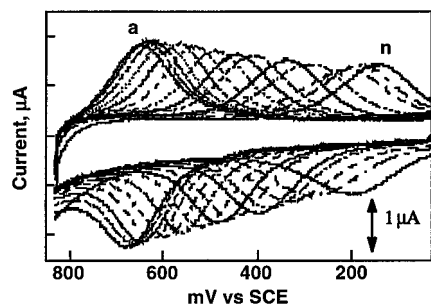
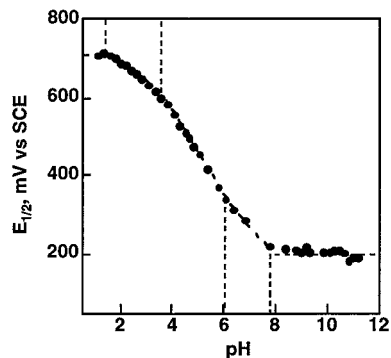**Figure 4.** Cyclic voltammograms of the mixed [Ru(dtbimpy)(bimpyH₂)]-(PF₆) SAM prepared from the solution containing both the Ru(II) complex and octanethiol as a diluent in different pH solutions at a scan rate of 0.2 V/s on a gold electrode. The mole fraction of the Ru(II) complex in the solution is 0.88, and the total molar concentration of the Ru complex and diluent thiols is 0.35 mM. Voltammetric curves a—n were obtained at pH values of 1.33, 1.83, 2.21, 2.59, 3.10, 3.58, 4.09, 4.52, 4.86, 5.36, 5.83, 6.35, 6.88, and 7.35, respectively.

(tppz)]²⁺, where L18 = 2,6-bis(1-octadecylbenzimidazol-2-yl)-pyridine) and tppz = 2,3,5,6-tetrakis(2′-pyridyl)pyrazine, at the air−water interface.[29] In the case of the mixed Ru SAM with octanethiol, two peaks, I and II, are shifted in the opposite direction; i.e, peak I is shifted in the negative direction, but peak II moves in the positive direction as shown in Figure 3. This dilution experiment reveals the formation of a homogeneously mixed monolayer between the Ru complex and the octanethiol on the gold surface. From these data, we proposed the Ru SAM forms a well-ordered domain structure at the early stage, then a disordered structure is formed, and reorganization occurs at the domain boundary. Domain formation has been reported in the reductive desorption of a binary SAM with different lengths of the alkyl chain and different types of terminal groups.[36]

The cyclic voltammograms for a gold electrode of the Ru-(II) complex with diluent octanethiol solution were obtained in solutions of different pH values (Figure 4). At slow sweep rates (typically 0.2 V s⁻¹), all cyclic voltammograms display characteristics of a surface-confined redox process corresponding to Ru(III/II). On each cyclic voltammogram (CV), the integrated charges of the anodic peak and the cathodic peak are identical within experimental error and the wave shape is quite symmetric ($\Delta E_p = 20-40$ mV). These characteristics of each CV are maintained when the pH is varied from 1.12 to 7.35. In this study, the potential shift due to pH change in the monolayers is totally reversible; however, the surface coverage decreased to 80−90% compared to that of the initial state. The half-wave potential of each CV was plotted with the pH of the electrolyte solution (Figure 5).

Over the range of pH 3.5−5.9, $E_{1/2}$ decreases with a slope of −110 mV/pH as pH increases. In this range, the redox reaction of the Ru(II) complex is a reversible two-proton, one-electron process. However, $E_{1/2}$ decreases linearly with a slope of −55 mV/pH as the pH increases in the range pH 5.9−8.0. In this interval, the redox reaction of the Ru(II) complex is a reversible one-proton, one-electron process. Below pH 2 and above pH 8, a zero slope was observed. At this stage, two NH imino protons of a surface-immobilized Ru(III/II) couple are fully protonated or deprotonated, respectively. Therefore, no proton-coupled electron-transfer process takes place in these regions.

(34) Haga, M.; Wang, K.; Monjushiro, H. Manuscript in preparation.
(35) (a) Imabayashi, S.; Hobara, D.; Kakiuchi, T.; Knoll, W. *Langmuir* **1997**, *13*, 4502. (b) Yang, D.-F.; Wilde, C. P.; Morin, M. *Langmuir* **1997**, *13*, 243.
(36) Bard, A. J.; Faulkner, L. R. *Electrochemical Methods. Fundamentals and Applications*; John Wiley & Sons: New York, 1980.

Figure 5. Half-wave potential ($E_{1/2}$) for the mixed Ru SAM film vs solution pH.

Scheme 4. Proton-Coupled Electron-Transfer Reaction of the [Ru(dtbimpy)(bimpyH₂)] SAM Complex Immobilized on the Polycrystalline Au Surface in Three Different pH Regions
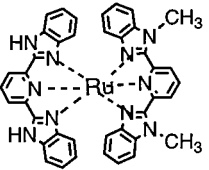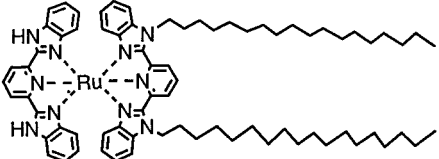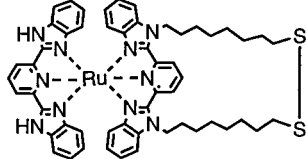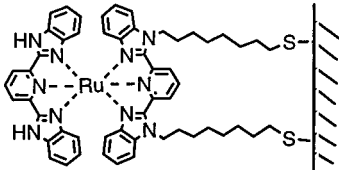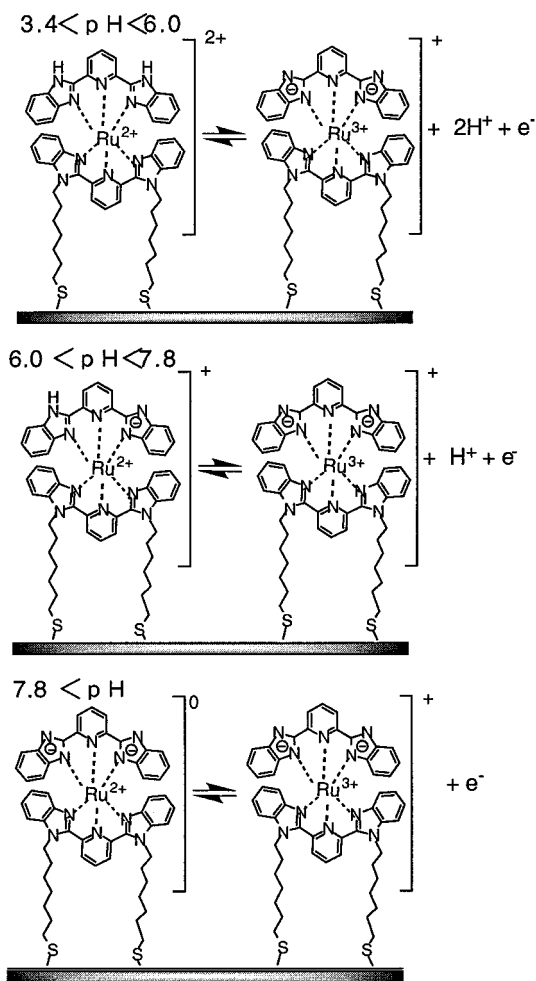

The consecutive ionization of two imino protons of the benzimidazole ligand of the Ru(II) complex on the gold electrode results in a dramatic shift of $E_{1/2}$ by 0.5 V with changing pH from 2 to 8. The proton-coupled electron-transfer reaction in the immobilized Ru complex on the Au surface can be summarized in Scheme 4. The breakpoint of two lines in the plot of $E_{1/2}$ vs pH gives the pK_a values of pK_{a1} = 6.0 and pK_{a2} = 7.8 for the Ru(II) state and ~1.5 and 3.4 for the Ru(III) state. These pK_a values for the SAM are a little smaller than those in a CH₃CN/buffer solution (Table 1). The effect of diluent octanethiol on the pK_a values obtained from the Pourbaix

Table 1. Summary of pK_a Values of [Ru(L)(bimpyH$_2$)]$^{2+}$ in Different Microenvironments

Complex	Condition	pK_a values pK_{a1}	pK_{a2}
	In CH$_3$CN/buffer[a]	6.35 ± 0.05	7.87 ± 0.05
	In 10 mM Triton /0.1 M Na$_2$SO$_4$ (in micelle condition)[a]	5.35 ± 0.05	6.94 ± 0.05
	In CH$_3$CN/buffer[a]	5.70 ± 0.05	7.33 ± 0.05
	In CH$_3$CN/buffer[b]	6.0 ± 0.1	7.8 ± 0.1

[a] From UV spectrophotometric titration. [b] From electrochemical Pourbaix diagram.

diagram could not be obtained because the cyclic voltammogram of the neat Ru SAM electrode was drawn out when the solution pH increased. Therefore, we could not determine the accurate pK_a values on the neat Ru SAMs. The strong intermolecular interaction in the domain microenvironment may be responsible for this behavior.

To describe the ion distribution in the SAM/solution interfaces, the Gouy–Chapman theory can be applied. The electrostatic potential, $\Psi(z)$, between the monolayer surface and the bulk solution induces a shift in the localized pH according to the following equation:[36]

$$\text{pH}(\infty) = \text{pH}(z) + \frac{e\Psi(z)}{2.3kT}$$

$$\Psi(z) = \frac{2kT}{ze}\sinh^{-1}\left(\frac{\sigma^M}{(8kT\epsilon\epsilon_0 C)^{1/2}}\right)$$

where pH(∞) and pH(z) are the bulk and near the interface pH values, σ^M is the charge density at the monolayer surface, C is the concentration of the electrolyte, ϵ is the dielectric constant of the medium, and ϵ_0 is the permittivity of free space. If we assume that all the charge on the surface is associated with the present Ru(II) complex in the mixed SAMs ($\sigma^M = zF\Gamma$, where $\Gamma = 0.8 \times 10^{-10}$ mol/cm^2 and $z = +2$), we can obtain the electrostatic potential, $\Psi(z) \approx 80$ mV, which is equivalent to a 1.3 pH unit increase in local pH. This effect would be reflected in a decrease of pK_a values in comparison with those of the bulk phase. Furthermore, the double-layer model predicts that the pK_a values shift in the negative direction when the loading of the Ru complex increases. Our attempts to obtain the Pourbaix

diagram for the neat Ru SAMs failed so far, because the strong intermolecular interaction in the neat Ru SAMs makes it difficult to obtain well-behaved voltammograms over a wide range of pH. Since a small decrease of pK_a values was observed in the present mixed SAMs with octanethiol compared with that in bulk solution (Table 1), the experimental difference between surface and bulk pK_a values does not agree well with the predicted value from the Gouy–Chapman double-layer theory.[6] The discrepancy between observed and predicted ΔpK_a values may arise from too much simplification of the surface structure in the present Ru SAM system for applying the double-layer theory.

Several studies of the proton-coupled electron-transfer system on the surface have been reported.[4,6] Observation of a dramatic increase in the pK_a value of a flavin analogue SAM on gold compared with that in bulk solution was explained by the interfacial potential effect.[4] These results are in line with the observation of Whitesides et al., who demonstrated increased pK_a values of acidic groups of ω-mercaptoalkanecarboxylic and phosphonic acids self-assembled on gold surfaces.[18,37] On the other hand, it has been reported that the variation of $E_{1/2}$ with pH for the Ru(III/II) surface couple of [Ru(tpy)(4,4'-(PO$_3$H$_2$)$_2$-bpy)(H$_2$O)](ClO$_4$)$_2$ overlays the dependence of the solution couple.[6]

As mentioned above, $E_{1/2}$ does not change when the solution pH is set below 2. However, the peak potential began to shift in the negative direction once again when the molar concentration of HClO$_4$ increased below pH 1. In the concentration range of 0.1–3.0 M HClO$_4$, a linear plot with a slope of 52 mV per

(37) Bain, C. D.; Whitesides, G. M. *Langmuir* **1989**, *5*, 1370.

unit in log [HClO$_4$] was obtained. Such a potential shift was not observed in concentrated HCl solution. In the strong acidic solution of HClO$_4$, this shift of the half-wave potential presumably results from the formation of ion pairing between Ru(III) and perchlorate anion upon oxidation of the Ru(II) complex. The propensity of ClO$_4^-$ to form ion pairs with ferrocinium cation has been reported on self-assembled monolayers of ferrocenethiols.[16,25]

In conclusion, we have prepared a novel Ru-2,6-bis(benz-imidazol-2-yl)pyridine SAM immobilized on a Au surface, which shows proton-coupled electron-transfer reactions. The available potential range is about 0.5 V wide with a pH change from 2 to 8. The ability for reversible tuning of a surface formal potential in redox-active Ru SAMs plays a key role in designing a gate material for proton and electron transfer or an electrochemical proton generator.

Supporting Information Available: XPS core level spectra for the Ru complex, MALDI spectrum of the [[Ru(dtbpim)(bpbimH$_2$)] SAM complex immobilized on a polycrystalline Au surface, cyclic voltammograms of [Ru(dmbimpy)(bimpyH$_2$)](PF$_6$)$_2$ in CH$_3$CN/buffer (1:1 v/v) solution in the pH range from 2.70 to 7.81, and a plot of the half-wave potential vs log [HClO$_4$] for Ru SAM monolayers. This material is available free of charge via the Internet at http://pubs.acs.org.

IC990934S